7 September 1984, Volume 225, Number 4666 SCIENCE

Packing Structures and Transitions in Liquids and Solids

Frank H. Stillinger and Thomas A. Weber

Summary. Classification of potential energy minima—mechanically stable molecular packings—offers a unifying principle for understanding condensed phase properties. This approach permits identification of an inherent structure in liquids that is normally obscured by thermal motions. Melting and freezing occur through characteristic sequences of molecular packings, and a defect-softening phenomenon underlies the fact that they are thermodynamically first order. The topological distribution of feasible transitions between contiguous potential minima explains glass transitions and associated relaxation behavior.

For reasons still imperfectly understood, periodic crystalline order provides the most stable arrangement for the molecules of pure substances in bulk. This circumstance has caused crystallography to become and to remain one of the most powerful tools available for revealing the structure of molecules and the nature of intermolecular forces.

Perfect crystals are a rarity in our environment. More typically, dense matter appears as defective crystals, amorphous solids, and liquids. Describing the corresponding spatial arrangements of atoms and molecules is a major challenge on account of the diversity of possibilities and because no experimental technique or combination of techniques currently provides the necessary atomic-level precision and resolution comparable to those in crystallography. Nevertheless, compelling scientific and technological needs continue to demand just that kind of structural information.

The spatial patterns of atoms in crystals and in amorphous solids share a basic attribute, at least at low temperature, where vibrations are minimal. It is that both represent minima in Φ, the potential energy function that describes interactions in the respective systems. Perfect crystals correspond to absolute minima, defective crystals to higher relative minima, and amorphous deposits to minima that are higher still. This article explores some general facts about such locally stable minima, focusing in particular on their nonobvious relation to and influence on the liquid phase (*1*). The resulting conceptual framework seems to be useful for understanding a broad range of chemical and physical phenomena in condensed phases.

Mapping onto Minima

Figure 1 illustrates in highly schematic fashion a small portion of the multidimensional potential energy surface for an N-atom system. This drawing compresses into a two-dimensional cartoon the $3N$-dimensional function Φ of all atom positional coordinates. The constant-Φ curves shown encircle various local minima (filled circles). Neighboring pairs of minima are separated by saddle points (crosses) through which minimum-barrier paths would pass in connecting those minima. In general Φ will comprise internal interactions in the collection of atoms, such as chemical bonds and van der Waals forces, and external interactions with vessel walls. Included somewhere in this collection of minima are the absolute minima corresponding to crystalline arrangements of the atoms.

For any but the smallest values of N the number of distinct Φ minima is impressively large. First, there is permutation symmetry to contend with: if all N atoms are identical, every local minimum belongs to a family of $N!$ minima all of the same depth and differing only by atom interchanges. Second, the number of geometrically distinguishable families of minima will rise exponentially with N. This latter feature rests on the expectation that particle packings can be rearranged essentially independently in the two halves of a large system. Precise values of these numbers of distinguishable minima are elusive, but one estimate (*2*) suggests that 1 gram of argon at its normal liquid density would possess roughly $10^{10^{22}}$ distinguishable particle packings.

To understand condensed phase properties systematically in terms of Φ minima it is necessary first to carry out a division of the multidimensional space depicted in Fig. 1. The purpose is to assign any configuration of atoms uniquely to one local minimum; if it is not already at a minimum the displacement exhibited by the system is simply regarded as a "vibrational" displacement, possibly anharmonic in character. Thus packing and vibration effects can in principle be cleanly separated.

The procedure for carrying out this division is straightforward if all atoms involved are identical (*3*). Any arbitrary configuration is assigned to the minimum that is finally encountered when moving "downhill" from that starting point along a steepest descent direction. Technically, this means that configurations

The authors are members of the technical staff in the Chemical Physics Department, AT&T Bell Laboratories, Murray Hill, New Jersey 07974.

are connected to (mapped onto) minima by solutions to the multidimensional equation

$$\partial \mathbf{r}/\partial s = -\nabla \Phi(\mathbf{r}) \quad (1)$$

where the vector $\mathbf{r}$ comprises all $3N$ atomic coordinates and where s is a virtual "time coordinate" for the descent (*4*). Starting at any randomly chosen $\mathbf{r}(s = 0)$, the solution $\mathbf{r}(s)$ as $s \to \infty$ locates the requisite minimum. The dotted lines in Fig. 1 outline the regions containing all points that map onto the same interior minimum. Notice from Fig. 1 that boundaries separating neighboring regions pass through saddle points on the Φ hypersurface.

Having introduced this division of the configuration space, a primary goal will be to describe motion within and transitions between the regions and how that motion depends on temperature.

Computer Simulation

The complicated topography of the Φ surface (Fig. 1) profoundly influences experimental measurements for the substance under consideration. But such measurements have very limited capacity to determine the topography and to follow details of the system's dynamical motion across the "Φ-scape." Digital computer simulation offers an insightful alternative, at least for small (and one hopes representative) collections of 10^2 to 10^3 atoms. Our own work in this area has relied on a computer to solve classical Newtonian equations of motion, subject to suitable initial and boundary conditions, with analytical potential functions that have been selected to represent specific materials of interest. As the classical dynamical trajectory is being generated the computer is required to carry out in parallel and frequently another set of tasks, namely to identify the Φ minimum onto which the instantaneous dynamical configuration would map by the steepest-descent construction (Eq. 1). This parallel activity supplies a running record of the fiducial minima over whose regions the Newtonian dynamics takes the system. This would be analogous to a listing of names of counties passed over during a transcontinental flight from New York to San Francisco.

If initial conditions for the dynamics so decree, the system can be trapped at low total energy in the neighborhood of a single minimum. In that event the mapping yields a consistently monotonous result. But at higher energy, escape over saddle points becomes possible and the running mapping onto minima reveals kinetic details about transitions between contiguous regions. Figures 2 and 3 provide a case in point. They refer to a computer simulation for an amorphous alloy at low temperature (174 K) comprising 120 nickel atoms and 30 phosphorous atoms. Figure 2 shows how the potential energy per atom, ϕ, varies with time during a 3.1-picosecond interval, along the classical dynamical trajectory executed by this 150-atom system in its 450-dimensional configuration space. The thermal motion of the atoms in this solid deposit consists primarily of harmonic motion; but more than that is

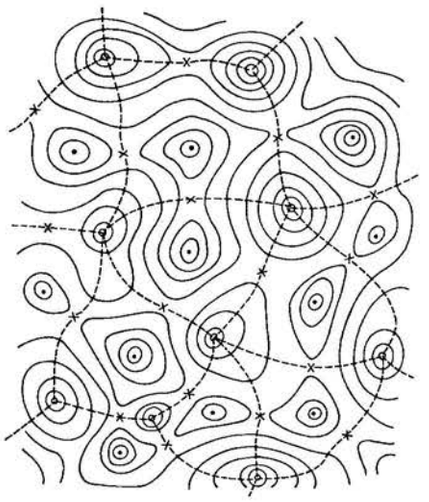

Fig. 1. Schematic representation of the potential energy surface for an N-atom system. Minima are shown as filled circles and saddle points as crosses. Potential energy is constant along the continuous curves. Regions belonging to different minima are indicated by dashed curves.

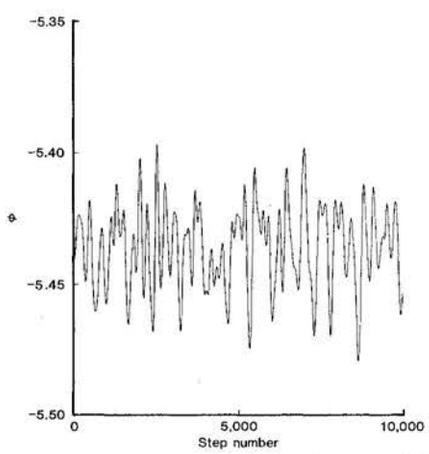

Fig. 2. Time variation of ϕ, the potential energy per atom, in a 150-atom nickel-phosphorous amorphous deposit, as simulated by computer. Temperature is 174 K. The 10^4 computer time steps shown correspond to 3.1 picoseconds of elapsed time. The quantity ϕ is shown on a reduced basis; the energy unit used is 1.855 kilocalories per mole.

present. Figure 3 shows, for exactly the same interval, the value of ϕ at the nearby potential energy minima. Obviously the system has not merely executed vibrations around a single minimum but has undergone ten transitions between neighboring minima. In this case all the minima visited correspond to amorphous packings of the given set of atoms.

If the temperature is increased for the nickel plus phosphorus system to which Figs. 2 and 3 refer, the transition rate between regions surrounding distinct minima increases dramatically. This temperature-dependent rate can be analyzed with an Arrhenius plot (logarithm of rate versus $1/T$) to estimate the mean barrier height. For the few cases that have been carefully examined this way, the mean barrier height for liquids turns out only to be about half of that which emerges from a corresponding Arrhenius plot for self-diffusion rates. The implication is that many transitions "get nowhere," that is, either involve motion into and out of culs-de-sac in the configuration space or must dynamically be followed by a surmounting of higher bottleneck barriers for diffusion to occur.

Certainly, computer modeling of bulk matter involving only 10^2 to 10^3 atoms requires care in interpretation. Nevertheless, the modest kinds of mapping-to-minima calculations just illustrated apparently produce several results of general validity. Included among them are the following:

1) Transitions are localized. The atomic arrangements for two successively visited packings (such as those indicated in Fig. 3) normally differ only by rearrangement of a small set of atoms that form a compact grouping in three-dimensional space. Most of the material present stays put, or at most responds elastically to the local rearrangement. Evidently, overall restructuring requires a sequence of many localized transitions.

2) The transition rate is an extensive quantity, that is, the rate is proportional to the system size at least in the macroscopic limit. This feature follows from point 1 above. By doubling the size of the system (while holding temperature and composition fixed), the number of sites at which localized transitions could occur also doubles. Consequently, the mean residence time in any given minimum region becomes halved. In conjunction with results from small-system computer simulation, this extensivity requires truly formidable transition rates for macroscopic samples of matter. For example, one estimate (*2*) implies that 1 mole of liquid argon near its melting

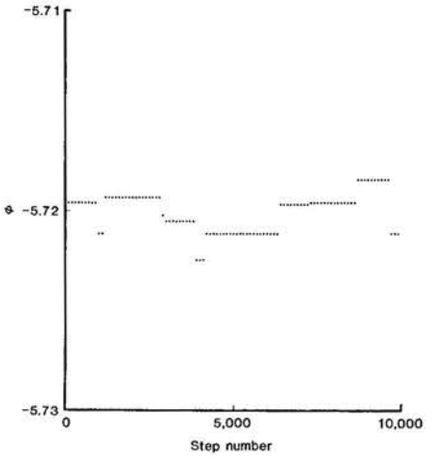

Fig. 3. Time variation of ϕ at potential minima for the amorphous nickel-phosphorus system represented in Fig. 2. The results shown were obtained by numerically solving the mapping-to-minima equations every 100 time steps (0.031 picosecond). The same units are used here as in Fig. 2.

point (84 K) has a mean residence time in each minimum of only 7×10^{-36} second. Nevertheless, rearrangements in any fixed molecular locale will (by point 1) occur at a rate independent of system size.

3) Only a small fraction of the direct transitions entail permutations of identical particles. Such transitions would involve concerted motion of identical atoms around a closed loop and would have equivalent initial and final packings. For the most part it is found that particle exchanges occur as a result of several successive transitions, no one of which is purely permutational. It has been inferred from computer simulation on a model for liquid argon that only about 3 percent of the direct transitions are permutational (*2*).

4) When plotted against ϕ, the potential energy per atom, the statistical distribution of distinguishable minima is strongly peaked at a value corresponding to amorphous packings. Furthermore, the distribution is markedly skewed toward the low-ϕ direction. This asymmetry owes its existence to the possibility of crystallinity. There is no such thing as an "anticrystal" to provide packings correspondingly far from the distribution maximum but to the high-ϕ side. The typical distribution is shown in logarithmic form in Fig. 4. For substances that have a conventional first-order melting transition, Fig. 4 shows that inhomogeneous (partly crystalline, partly amorphous) packings will dominate the distribution in the intermediate ϕ range.

5) When the system dynamics moves through the collection of regions for the amorphous packings, the direct transitions can have arbitrarily small barriers and can involve arbitrarily small changes in Φ from one minimum to the next. In particular, there exists a distribution of small-barrier and small-bias transitions in all amorphous deposits that have been modeled by computer simulation. This observation has significance, since virtually all amorphous solids experimentally show thermal and kinetic behavior at very low temperatures, indicating the presence of quantized "two-level systems" (*5*). According to Anderson *et al.* (*6*) and Phillips (*7*), these are atoms or localized groups of atoms that are bistable; a collective coordinate describing their translocation is such that it causes Φ to pass over a low barrier between closely spaced minima. The molecular dynamics computer simulation is classical, of course. But it provides a means for determining what groups of atoms create local bistability and how they move from one position to the other along the collective coordinate. These are details that experimentation is hard-pressed to supply for real amorphous materials, but which are a basic prerequisite to a microscopic quantum theory of amorphous solids.

6) Provided that the temperature is at or above the melting point temperature T_m (so that the system is a thermodynamically stable liquid), the minimum-region sampling yields a distribution that depends on density but is very nearly independent of temperature. As was stressed above, the rate of sampling is strongly dependent on temperature. But if density is held constant, the distribution of minima actually visited in the dynamical evolution of the system is virtually always the a priori distribution schematically illustrated in Fig. 4. That this is so hinges on the fact that the dominating amorphous minima are narrowly distributed in potential energy on a per-atom basis relative to the thermal energy k_BT. Consequently, thermal bias across this narrow distribution is virtually negligible.

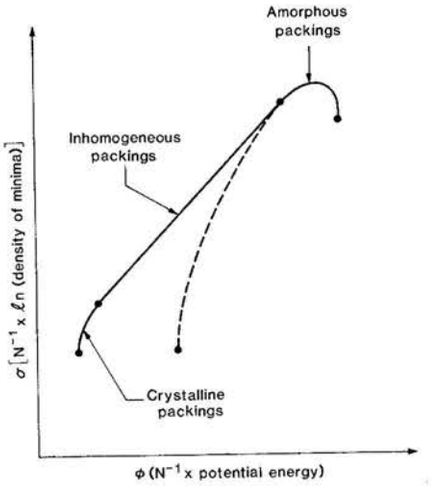

Fig. 4. Logarithm of the distribution of potential energy minima, plotted against potential energy per particle. The case shown corresponds to a pure substance that has a first-order melting transition.

Inherent Structure in Liquids

Short-range order in liquids and amorphous solids conventionally is analyzed and discussed in terms of the pair correlation functions $g_{ij}(r)$ for atomic species i and j. These are defined to be proportional to the number of i,j pairs with separation r present in the system, with a normalization such that each g_{ij} approaches unity for large r. In a pure elemental substance there is only one such function and it can be determined experimentally by x-ray or neutron diffraction. When two or more atomic species are present the independent g_{ij} can be extracted only by an adroitly chosen combination of x-ray and neutron diffraction experiments, with the latter utilizing one or more distinct isotopic compositions (*8*). The $g_{ij}(r)$ experimentally are found to vary with temperature, showing as expected more short-range order at low temperature than at high temperature. This variation in the liquid phase seems to invite interpretation as shifting equilibrium between various competing structures in the medium.

Point 6 above offers an important conceptual simplification for interpreting the g_{ij}. Suppose that the mapping onto minima has been carried out from a representative set of configurations selected from a liquid at temperature T above its melting point. In principle the resulting collection of static packings can themselves be used to calculate their own "quenched" pair correlation functions $g_{ij,q}(r)$. Point 6 implies that this new set of correlation functions should be virtually independent of the starting temperature. The difference between g_{ij} and $g_{ij,q}$ is simply that the former possesses a variable extent of thermal vibration away from potential minima, a phenomenon totally absent in the latter. Consequently, the $g_{ij,q}$ should reflect the presence of a T-independent inherent structure in the liquid phase.

This hypothesis for the liquid state has been tested and found valid for monatomic substances by computer simulation. Specifically, models for liquified noble gases and molten alkali metals have been examined (*9, 10*). It also ap-

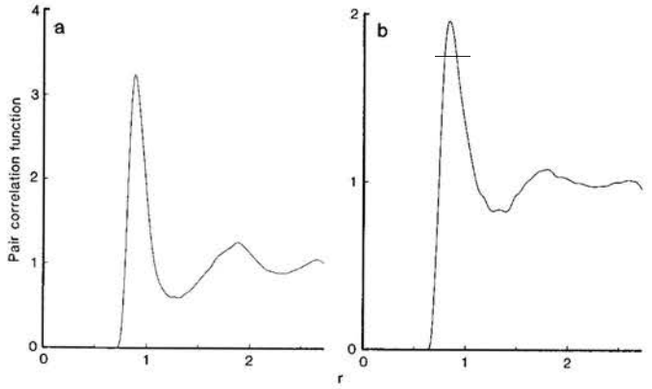

Fig. 5. Mixed-species pair correlation functions for the nickel (80 percent) plus phosphorus (20 percent) mixture (computer simulation). Two temperatures above the eutectic freezing temperature (1153 K) are shown: (a) 1223 K and (b) 6881 K. Both cases have mass density of 8.358 grams per cubic meter.

pears that mixtures satisfy the hypothesis as well. Figure 5 shows the pair correlation function $g_{NiP}(r)$ for the nickel-phosphorus alloy system evaluated at two temperatures, one just above the eutectic and one much higher. Figure 6 shows the common function $g_{NiP,q}(r)$ that arises from both after mapping onto the corresponding sets of potential energy minima. One advantage of this procedure is immediately obvious from Fig. 6. The first peak has become strongly sharpened and completely detached from the remainder of the correlation function, leading to an unambiguous identification of the mean nickel coordination of the sparse phosphorus atoms as 7.07.

Although inherent pair correlation functions are not directly observable in the laboratory, in some cases it should be possible to carry out sufficiently rapid quenches of liquids to approach $g_{ij,q}$. The mapping operation defined by Eq. 1 permits no annealing (hopping over potential energy barriers). This suggests that pair correlation functions should be measured near 0 K for sets of samples quenched at various rates from the liquid state. The inherent pair correlation functions $g_{ij,q}$ would then be obtained as the infinite quench rate limit of these results.

The existence of inherent structure in liquids has not been anticipated by molecular theory of liquids (*11*). Consequently, an important challenge to theory now exists to predict the $g_{ij,q}$ from first principles and to show how the directly measurable quantities g_{ij} can be reconstituted by application of suitable thermal broadening to $g_{ij,q}$. First indications are that this reconstitution process must be complicated on account of anharmonicity: attempts to reproduce g_{ij} from $g_{ij,q}$ by application of harmonic-oscillator broadening (in both Einstein and Debye oscillator models) fail.

While the existence of a T-independent inherent structure may well characterize most stable liquids, there might be one important exception. This involves liquid mixtures near consolute (critical unmixing) points, for example CCl_4 and n-C_7F_{16} for which the critical temperature is 28.6°C (*12*). As such a system approaches its consolute point, long-range fluctuations in composition appear, a natural symptom of critical point behavior (*13*). These fluctuations will produce correspondingly long-range modifications in the pair correlation functions g_{ij} that probably will survive the mapping onto potential minima. Consequently, $g_{ij,q}$ will or will not also exhibit long-range critical correlations depending on whether the starting state was or was not in the critical solution region, an obvious T-dependent factor.

Melting and Freezing

The distinctions between molten and crystalline states of the same substance are clear to the most casual observer. Virtually all measurable properties undergo discontinuities upon melting or freezing, with the sudden change of fluidity to rigidity being perhaps the most obvious. Understanding how and why these discontinuities occur in terms of potential energy minima leads to new and useful insights.

To discuss melting and freezing transitions effectively, we need an expression for the Helmholtz free energy F in terms of properties of the minima. The general theory of potential minima and their surrounding regions (*3*) supplies the following exact variational expression for a single-component substance:

$$F = F_0(T) + N \min\{\Phi + f_v(\phi,T) - k_B T\sigma(\phi)\} \quad (2)$$

Here N is the number of particles (atoms or molecules), k_B is Boltzmann's constant, and F_0 is an additive part of the free energy that is irrelevant for present purposes. The natural logarithm of the density of minima, the quantity plotted in Fig. 4, is denoted here by $\sigma(\phi)$. The mean vibrational free energy for those regions whose minima lie at $\Phi = N\phi$ is the quantity f_v. The minimum indicated in Eq. 2 is that which obtains when ϕ is varied at constant temperature and volume.

In the high-temperature limit the minimum in Eq. 2 will be determined solely by the last term and will occur at the maximum of $\sigma(\phi)$. As temperature declines, $\phi + f_v$ exerts an influence that displaces the minimum to lower ϕ. On account of the narrowness of the distribution near its maximum, this displacement remains small while the system is still in the molten state; this is the characteristic that leads to the inherent liquid structures discussed in the previous section. Eventually, declining temperature displaces the minimum of the expression in Eq. 2 to the lowest possible ϕ value, namely that corresponding to the perfect crystal. The liquid-crystal transition must intervene between these limits.

The simplest forms of structural disorder in an otherwise perfect crystal appear as point defects, specifically vacancies (missing particles) and interstitials (extra particles). These elementary structural excitations have been observed by the molecular-dynamics-with-mapping technique to appear spontaneously as separated vacancy-interstitial pairs when the crystal is held for relatively long periods of time near its melting temperature (*14*). After being created these defects are able to diffuse. But while the crystalline phase is thermodynamically stable, the concentration of these defects is very low; typically, one crystal site in 10^4 is occupied by a point defect.

There is evidence that on average the defects exert an attraction for one another. In the very dilute gas of defects characteristic of the crystal at thermal equilibrium, this is a negligible effect. But the concentration of defects can be markedly increased, for example by superheating the crystal. At a sufficiently high concentration of defects the mean attraction becomes a dominating influence. The defect gas then spontaneously condenses to produce a medium that is everywhere defective, namely the amorphous packings discussed above. This is how melting occurs. Inversely, freezing can be described as cavitation and evaporation of the dense defect medium. These transformations are illustrated in Fig. 7.

The mean attractive force between point defects may be viewed in another way, namely that a defect-softening phenomenon operates in the initially crystalline medium. Quantitative studies of packings show that as vacancy-intersti-

tial pairs are inserted into the crystal, the amount of reversible work that must be expended for each successive pair declines. In other words, the medium becomes easier to deform as it becomes more defective. Defect softening can also be quantitatively documented by examining calculated normal mode frequencies for packings that contain various concentrations of defects. It is found that the mean frequency, as judged by vibrational free energy in the harmonic approximation, tends to be lowered by an increasing concentration of defects. The implication is that the quantity $f_v(\phi,T)$ in Eq. 2 decreases smoothly when (at constant T) ϕ increases from the crystalline lower limit to the fully amorphous upper limit. To the extent that experimental comparisons are possible between crystalline and amorphous solid forms of the same substance, defect softening seems to be an empirical fact: elastic constants, for example, are reduced by transforming matter from crystalline to amorphous (*15*).

Referring once again to Fig. 4, we see the indication that, in the intermediate ϕ regime (between nearly perfectly crystalline and fully amorphous), the dominant packings are inhomogeneous. This is simply a reflection of the mean attraction–induced condensation of defects. For these values of ϕ the overwhelming majority of the particle packings have most of the defects clustered together in an obviously amorphous portion of the system, while the remaining portion is crystalline and nearly defect-free. This situation is illustrated qualitatively by the bottom diagram in Fig. 7. At the given intermediate ϕ there are simply many more ways to create packings with a large number of inhomogeneously distributed defects than with a smaller number of homogeneously distributed defects.

Information extracted from computer simulation studies can be assembled into a statistical-mechanical theory of defect-mediated melting. The specific ingredients required are the defect-pair formation energy, defect-softening effects on mean attraction between defects and on vibrational free energy, and a specification of the types of allowable defect arrangements that are consistent with mechanical stability of the packing. This is not an appropriate place to dwell on details, but it is illuminating to cite one example, namely the melting transition for a model of the alkali metals. For these substances, which crystallize in the body-centered cubic structure, the appropriate partition function has been derived in terms of the packings with variable defect concentrations (*14*). The

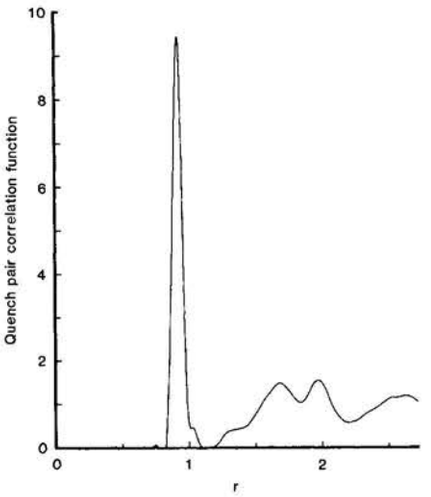

Fig. 6. Common mixed-species pair correlation function $g_{NiP,q}$ calculated from collections of stable packings for the liquid states involved in Fig. 5.

corresponding version of variational Eq. 2 has then been solved to find $\phi_m(T^*)$, the mean packing potential energy, and $\theta(T^*)$, the degree of saturation of the packings with defects, for variable reduced temperature T^*. The results for the latter function are displayed in Fig. 8. The solid curve corresponds to thermodynamic equilibrium, with a vertical jump at the predicted melting temperature. Dashed extensions of the equilibrium branches refer to metastable supercooled liquid and superheated crystal. The return branch (dashed) is an unstable extremum of Eq. 2.

In Fig. 8 the predicted melting temperature agrees reasonably well with the direct computer simulation for the same model. This agreement lends credence to the analytical partition function on which the $\theta(T^*)$ curve is based. Equally significant is the fact that, over its entire stable range, the liquid phase remains almost completely saturated with defects [$\theta(T^*) > 0.998$]. More precisely, the packings that underlie the liquid are at all temperatures virtually the same fully amorphous set. This is yet another confirmation of the existence of a temperature-independent inherent structure for the liquid.

Compared to the melting temperature indicated in Fig. 2, the supercooling extension of the stable liquid branch is substantially longer than the superheating extension of the stable crystal branch. This is consistent with the common observation that liquid supercooling is indeed easier than crystal superheating for real materials.

Supercooling and Glass Transitions

When an undercooled liquid spontaneously nucleates and proceeds to freeze, its $3N$-dimensional configuration point passes through a characteristic sequence of packing regions. At first it wanders through those for homogeneously amorphous packings. Then it discovers an exit path into the inhomogeneous set, starting with those having just a small defect-free region (the critical nucleus). The portion of the momentary packing that is crystalline subsequently tends to grow until the entire packing is crystalline.

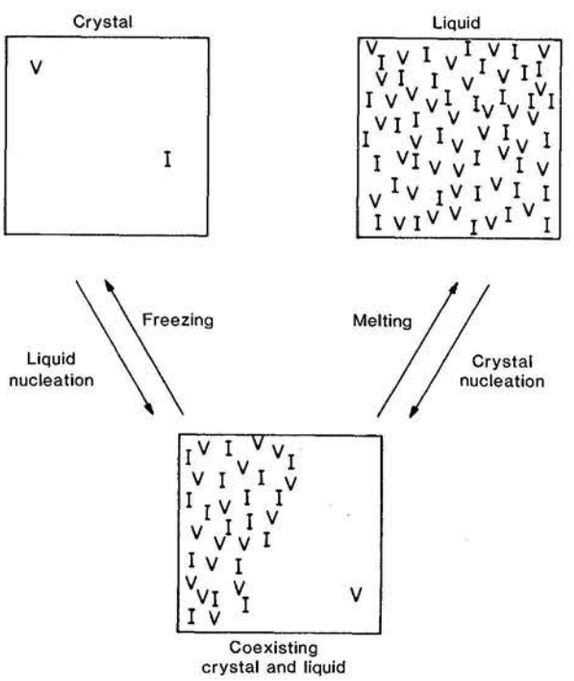

Fig. 7. Symbolic representation of melting and freezing transitions as condensation and evaporation, respectively, in the particle packings of the point-defect fluid. V and I stand for vacancy and interstitial; their relative concentrations depend on whether constant-volume or constant-pressure conditions apply.

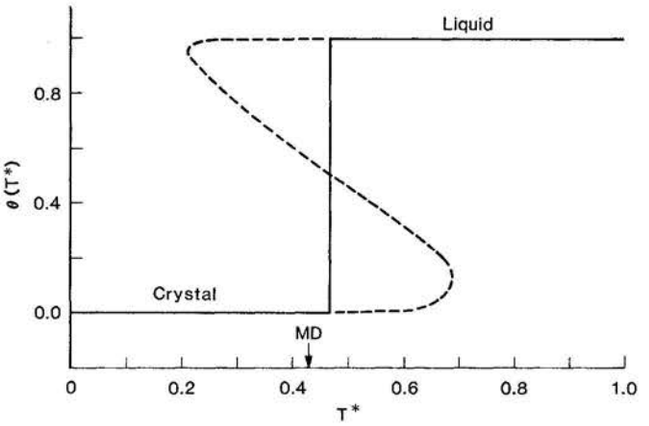

Fig. 8. Defect concentration in the particle packings versus temperature for melting of alkali metals. $\theta = 1$ corresponds to the maximum possible defect concentration. Thermal equilibrium values have been indicated by continuous curves and metastable extensions by dashed curves. These results are based on an analytical defect-mediated melting theory. Molecular dynamics (MD) calculations for the same underlying model produce a melting point.

However, this "normal" progression is often circumvented, either by extremely rapid cooling toward absolute zero or by selection of substances for which nucleation is especially improbable, even at slow cooling rates. The latter class of substances includes network-formers such as B_2O_3 and SiO_2, many nonrigid molecule organics such as glycerol and atactic polystyrene, and a wide variety of multicomponent liquid mixtures. For these, the $3N$-dimensional configuration point continues to wander through a subset of the collection of regions surrounding homogeneously amorphous packings. Exit to the inhomogeneous packing set is extremely unlikely, even when the system is cooled very slowly to absolute zero. The appropriate packing density σ_a to use in evaluating the free energy with Eq. 2 is just that for the homogeneous amorphous structures; this is indicated in Fig. 4 by the dashed curve. To the extent that homogeneously amorphous packings can unambiguously be distinguished from those with an inhomogeneous texture, the present theory at least formally offers a means for evaluating the thermodynamic functions of the supercooled liquid state.

Typically, easily supercooled liquids like those mentioned above become very viscous as temperature declines, and many display rather sharp glass-transition temperatures (*16*). This is the point at which kinetic processes in the fluid become so slow that equilibration, even within the restricted σ_a distribution, becomes infeasible. Properties become history-dependent and Eq. 2 ceases to supply a valid description. Explaining such behavior requires examination of the deep amorphous minima, their surrounding regions, and the transition states over which the $3N$-dimensional configuration point must pass for structural changes to occur.

The straightforward vacancy-interstitial description of disorder cited above for simple substances is not appropriate for the more complicated glass-formers. In fact, a proper description for these latter substances should be keyed to specific details of molecular size and flexibility, charge and polarity, and interaction directionality and additivity. Therefore, it should be no surprise that glass-transition behavior is nonuniversal, with a substantial range in the degree of sharpness of the "transition."

Nevertheless, some general observations seem to be in order. Figure 9 presents a transition map for homogeneously amorphous packings (those included in σ_a) of a glass-forming substance. Each filled circle represents a potential energy minimum, and lines connecting those circles stand for the feasible localized transitions that are available to the system. The vertical axis is the potential energy value, so indeed most circles are clustered and connected at a vertical position corresponding to the maximum in σ_a (and σ). However, the distribution of minima trails off toward the low-ϕ side, showing only a very sparse and widely separated set of minima at the low-ϕ limit. The minima labeled A and B are two such packings.

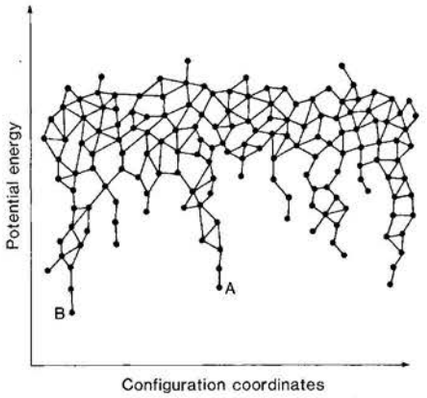

Fig. 9. Schematic drawing of the transition network for amorphous packings (symbolized as filled circles). A and B are a pair of low-potential amorphous packings.

Now consider what might reasonably happen as this system is cooled to low temperature. The random sequence of transitions during cooling should cause the system to enter and be trapped along one of the downward-hanging tendrils, such as that ending at A. The a priori chance that this is the tendril leading to the lowest potential minimum in the amorphous group, say B, is very small. To remain in thermal equilibrium the system at A must have kinetic access to B. However, the figure shows that such access requires a substantial backing up into considerably higher-ϕ packings. The energy and entropy of activation for such a sequence are clearly not those for any single transition, but are instead much larger and are determined by this backing-up phenomenon. Thermal equilibration is thus frustrated by dead ends. Structural relaxation is arrested, and the system exhibits its glass transition as the inevitable result.

Conclusions

The viewpoint advocated in this article shifts attention from ordinary three-dimensional space to the $3N$-dimensional realm where collective phenomena in condensed phases are determined. The existence and variety of potential energy minima in this multidimensional configuration space form a natural basis for quantitative study of those collective phenomena. Specific applications described here include the nature of short-range order in liquids, the melting and freezing transitions, and rate processes in low-temperature amorphous substances.

Results achieved thus far encourage extensions that could have widespread implications for chemistry, materials science, molecular biology, and condensed-matter physics. One of the most exciting prospects is development of a comprehensive theory of chemical reactions in the liquid phase. Provided that only ground-electronic states are involved, potential energy minima for reactive mixtures can be classified uniquely according to the numbers of solvent, reactant, and product species that are present. Reaction kinetics depends then on the average rate at which the dynamical

motion of the system causes transitions to occur between distinct classes of minima. From this perspective, the venerable absolute reaction rate theory (*17*) devised to describe activated chemical reactions in the gas phase would require generalization and modification to accommodate the distributions of minima and of transition states that appear in the present multidimensional description.

Biopolymer conformational problems continue to receive vigorous experimental and computational attention (*18*). The latter typically has involved a search for optimal conformations, that is, the absolute minimum of some postulated potential energy function that incorporates chemical bond lengths and angles, as well as more remote atom-pair nonbonding interactions. Solvation is usually disregarded, or at best incorporated in some simple averaged way. We conclude that the type of complete configuration space analysis outlined above (for biopolymers plus solvent) would be useful. First, it would help to assess the importance of solvent packing fluctuations. Second, consideration of the full distribution of potential minima would demonstrate how special the absolute minimum is geometrically. Third, examination of transition states would be enlightening with respect to annealing kinetics of suboptimal conformations to the absolute potential minimum. Systematic study of a few select cases could provide an important contribution to quantitative understanding of kinetic processes in molecular biology.

References and Notes

1. The scientific literature contains fragments of some of the basic ideas presented here. The reader's attention is directed to the following: J. D. Bernal, *Nature (London)* **183**, 141 (1959); H. Eyring, T. Ree, N. Hirai, *Proc. Natl. Acad. Sci. U.S.A.* **44**, 683 (1958); M. Goldstein, *J. Chem. Phys.* **51**, 3728 (1969); M. R. Hoare, *Adv. Chem. Phys.* **40**, 49 (1979).
2. F. H. Stillinger and T. A. Weber, *Phys. Rev. A* **28**, 2408 (1983).
3. ———, *ibid.* **25**, 978 (1982).
4. When atoms of different kinds are present, the terms on the left side of Eq. 1 must be weighted by the respective masses.
5. W. A. Phillips, Ed., *Amorphous Solids: Low-Temperature Properties* (Springer-Verlag, New York, 1981).
6. P. W. Anderson, B. I. Halperin, C. M. Varma, *Philos. Mag.* **25**, 1 (1972).
7. W. A. Phillips, *J. Low Temp. Phys.* **7**, 351 (1972).
8. J. E. Enderby, D. M. North, P. A. Egelstaff, *Philos. Mag.* **14**, 131 (1966).
9. F. H. Stillinger and T. A. Weber, *J. Chem. Phys.* **80**, 4434 (1984).
10. T. A. Weber and T. H. Stillinger, *ibid.*, in press.
11. J. P. Hansen and I. R. McDonald, *Theory of Simple Liquids* (Academic Press, New York, 1976).
12. D. R. Thompson and O. K. Rice, *J. Am. Chem. Soc.* **86**, 3547 (1964).
13. H. E. Stanley, *Introduction to Phase Transitions and Critical Phenomena* (Oxford Univ. Press, New York, 1971).
14. F. H. Stillinger and T. A. Weber, *J. Chem. Phys.*, in press.
15. D. Weaire *et al.*, *Acta Metall.* **19**, 779 (1971).
16. D. Turnbull, *Contemp. Phys.* **10**, 473 (1969).
17. S. Glasstone, K. Laidler, H. Eyring, *The Theory of Rate Processes* (McGraw-Hill, New York, 1941).
18. N. Gō, *Annu. Rev. Biophys. Bioeng.* **12**, 183 (1983).